

## Molecular marker approaches for tracking redox damage and protection in keratins

JOLON M. DYER, CHARISA D. CORNELLISON, ANITA J. GROSVENOR, STEFAN CLERENS, and SANTANU DEB-CHOUDHURY, Food & Bio-Based Products, AgResearch, Christchurch 8140, New Zealand (J.D., C.C., A.G., S.C., S.D.), Riddet Institute at Massey University, Palmerston North, New Zealand (J.D.), and Biomolecular Interaction Centre, University of Canterbury, Christchurch 8140, New Zealand (J.D.).

*Accepted for publication September 1, 2013.*

### Synopsis

There is increasing awareness of the importance of reductive and oxidative (redox) protein damage in protein-based materials including, hair, wool, nails, and skin. Light-induced damage to protein-based materials is of particular concern because of its impact on age-related degradation and product life spans. Consequently, cosmetic applications frequently target hair and skin restoration, where the integrity of the constituent filamentous proteins is essential to a healthy appearance. The keratins constitute an important subset of the structural proteins within skin, hair, and wool. We will introduce a means to assess damage to this important group of proteins at the molecular level, utilizing proteomic techniques to track the formation or degradation of sensitive peptides within intermediate filament proteins. The degradation of three molecular markers of redox damage, the peptides SFGYR, LASDDFR, and DVEEWYIR, along with the formation of their oxidized products, is demonstrated after exposure to ultraviolet A, ultraviolet B, and blue light. The method is shown to be suitable for evaluating the protective effect of treatments, as lower levels of oxidative markers were observed after the application of a protective fiber treatment. Molecular-level redox tracking will allow more targeted design and evaluation of protection and repair treatments for protein systems.

### INTRODUCTION

Keratins, previously also referred to as intermediate filament proteins, represent an important class of structural proteins of critical relevance to the physico-mechanical properties of mammalian fibers. Keratins are directly responsible for the structural integrity and associated physical and mechanical properties of hair, wool, skin, and nails (1,2). Both oxidative and reductive damages to these proteins result in deleterious effects, such as loss of strength and an increase in brittleness (3).

---

Address all correspondence to Jolon M. Dyer at [jolon.dyer@agresearch.co.nz](mailto:jolon.dyer@agresearch.co.nz).

Fibrous protein protection and repair technologies are becoming increasingly important in the formulation of functional hair and skin treatments. The evaluation of protein redox damage has traditionally been undertaken at a holistic level, such as through protein extraction assays or spectrophotometric carbonyl quantitation (4,5). However, for the targeted design, optimization and validation of next-generation protein protection and repair technologies, it is critical that robust and sensitive approaches for the evaluation of protein damage at the molecular level be developed and integrated with analysis at higher structural levels.

Here, we present the development and utilization of a peptide-based molecular marker approach for profiling and tracking oxidative damage in keratins, building on expertise in keratin degradation patterns (6,7). The approach is demonstrated using wool keratins, which have high sequence and structural homology with human hair and therefore represent a good model for evaluating the molecular-level effect of cosmetic treatments on keratins. Redox proteomic approaches were applied to characterize light-induced protein damage at the protein primary level in an enriched keratin extract and to track specific modifications across a range of irradiation conditions. Molecular markers characterized were then utilized to profile keratin damage to wool fibers both with and without the application of a protective silicon matrix fiber surface treatment, demonstrating the efficacy and sensitivity of our approach for evaluating protein protection.

## MATERIALS AND METHODS

Nonylphenol ethoxylate (trade name: Teric GN9) was obtained from Orica Ltd (Melbourne, Australia). Ethanol and urea were obtained from Merck Chemicals (Darmstadt, Germany). Thiourea was obtained from Sigma-Aldrich (St. Louis, MO); ChromAR® liquid chromatography (LC)-grade water and LC-grade acetonitrile, sodium tetraborate, and hydrochloric acid from J.T. Baker (Mumbai, India); and Univar formic acid from Ajax Finechem (Waltham, MA). Tris and sodium tetrathionate were obtained from BDH (Poole, UK). Sequencing grade trypsin was obtained from Promega (Madison, WI). Acrylamide was obtained from Bio-Rad Laboratories (Hercules, CA).  $\alpha$ -Cyano-4-hydroxycinnamic acid was obtained from Bruker Daltonics (Bremen, Germany). Nano-ES spray capillaries were obtained from Proxeon (Odense, Denmark).

*Wool preparation.* Mid-side wool samples from Romney fleece wool were detipped, then scoured and air-dried. This wool was cut into small sections, then freeze-crushed to a fine powder using liquid nitrogen in a mortar and pestle. The crushed wool sample was dried under vacuum over phosphorus pentoxide for 2 days. Whole wool samples were obtained in the form of woven, unbleached Merino wool fabric.

*Keratin extraction.* Dried wool powder was extracted overnight in tubes by vigorous shaking in a reciprocal shaker at room temperature in 0.1 M Tris, 0.2 M sodium tetrathionate, 0.1 M sodium tetraborate, and 8 M urea, pH 9.5 (HCl). Tubes were centrifuged to pellet the wool residue. The keratins were purified by precipitation and dialysis, and were then freeze-dried. Keratin purity was assessed by 2D gel electrophoresis, with no other wool protein classes observed.

*Whole wool surface photoprotection treatment.* Solgels were prepared as follows: Ethanol (6 ml) was added to 4.48 ml tetraethoxysilane and stirred for 30 min. Phenyltriethoxysilane (4.48 ml) was added, then 0.8 ml water was added dropwise, followed by 0.3 ml 10 M

HCl. The solution was kept stirring for 12 h (8). Wool fabric samples (6 cm × 6 cm) were treated with this silicon matrix solgel preparation by dip-coating for 5 min. The coated fabrics were allowed to dry overnight at room temperature and were annealed for 1 h at 120°C.

#### IRRADIATION PROTOCOLS

*Keratin irradiation.* Solid freeze-dried material was dissolved in water at 2 mg/ml and placed in ultraviolet (UV)-transparent quartz test tubes. The keratin solutions were irradiated with UVA, UVB, and/or blue light (9–11) for a period of 3, 24, or 72 h in an LZC4-14 photoreactor (Luzchem Research Inc., Gloucester, Ontario, Canada), at doses of 70,024 mWm<sup>-2</sup> (blue), 52,670 mWm<sup>-2</sup> (UVA), and 35,337 mWm<sup>-2</sup> (UVB).

*Whole wool irradiation.* Squares of untreated Merino wool fabric (3 cm × 3 cm) were treated with the solgel preparation and exposed to UVA and UVB irradiation (9–11) for varying periods to study the photoprotective efficiency of the matrix treatments. All experiments were run in triplicate.

*Color evaluation.* Squares of wool fabric treated with various silicon matrix preparations were exposed to UVA irradiation. Triplicate color measurements before and after UV irradiation were taken using a Minolta Chroma Meter CR210 (Osaka, Japan), with a wide area illumination, a 0° viewing angle, and a 50-mm diameter measuring area to average the reading over a wide area, as suitable for measuring cloth or textured surfaces. This yielded Y-Z values in CIE color space, which correspond very closely to yellowness as perceived by the human eye. A large Y-Z value indicates a very yellow sample.

*Digestion.* After irradiation, the wool was digested using an in-house established protocol: solubilization buffer (180 µl 8 M urea, 50 mM Tris, 50 mM tris(2-carboxyethyl)phosphine, 2 M thiourea, pH 8) was added to 6 mg of the wool and vigorously stirred overnight at 30°C. The extract was then alkylated with 360 mM acrylamide and the proteins from a 100 µl subsample were precipitated with 400 µl methanol, followed by 100 µl chloroform and then 300 µl water. The precipitate thus obtained was washed with 400 µl methanol, centrifuged at 14,100 g, and the methanol layer removed without disturbing the pellet. The pellet was suspended in 0.1 M ammonium bicarbonate–dimethylformamide (ratio: 7:3) and digested overnight at 37°C with trypsin (1:50), dried in a vacuum centrifuge, and stored at 4°C until further use. The tryptic peptides generated were desalted prior to direct infusion mass spectrometry (MS) with Proxeon StageTips (Proxeon, Denmark).

*Chromatography.* High-performance liquid chromatography (HPLC) analyses of the keratin digests were performed on a Bio-Rad BioLogic DuoFlow system equipped with a QuadTech multiwavelength UV-Vis detector, using a reversed-phase Bio-Rad RP-318 300 Å wide pore C18 column.

*Mass Spectrometric Analysis: Electrospray Ionization Tandem Mass Spectrometry.* Mass spectrometric analysis was performed on a tandem quadrupole-time-of-flight mass spectrometer (QSTAR Pulsar i, AB SCIEX, Framingham, MA), utilizing direct infusion nanospray of aqueous samples. LC-MS/MS was carried out on an Ultimate nanoflow HPLC equipped with Famos autosampler and Switchos column switching module (Dionex, Sunnyvale, CA). Subsamples (10 µl) were loaded on a C18 trap column (5 mm, 300 µm inner diameter) at

a flow rate of 8  $\mu\text{l}/\text{min}$ . The trap column was then switched in line with the analytical column (C18, 30 cm, 75  $\mu\text{m}$  ID). Both trap column and analytical column were in-house packed with Varian Microsorb C18 5  $\mu\text{m}$ , 300  $\text{\AA}$  particles. Reversed-phase gradients were from 2% to 55% solvent B at a flow rate of 150  $\text{nl}/\text{min}$  over 50 min. Solvent A was 0.2% formic acid in HPLC-grade water; solvent B was 0.2% formic acid in LCMS-grade acetonitrile. Loading and desalting solvent was 0.2% formic acid, 2% acetonitrile in HPLC-grade water. The analytical column outlet was directly connected to the mass spectrometer using a stainless steel nanospray needle (Proxeon). Triplicate technical repeats were performed for all samples.

## RESULTS AND DISCUSSION

### SELECTION OF MOLECULAR MARKERS

To characterize redox modification and select marker peptides for oxidative damage, a simplified system of enriched wool proteins was first evaluated. Type I and II keratins were isolated and purified from whole wool utilizing reductive sulfitylolyis (12). Solutions of these keratins were irradiated with UVA for periods between 0 and 72 h. The photo-modified proteins thus produced were enzymatically digested into peptide mixtures. Chromatographic analysis indicated substantial photomodification of the wool-derived proteins with increasing irradiation times, as demonstrated in Figure 1 (peptide oxidation is expected to result in an increase in UV absorbance due to the formation of UV-absorbing chromophores (13,14).

Electrospray ionization tandem mass spectrometry (ESI-MS/MS) was utilized to search for sequence-modified keratin-derived peptides and to characterize modifications corresponding to redox-modified residues. Certain residues, particularly the aromatic amino acid residues, were expected to be sensitive to UVA and UVB irradiation through type I and type II photooxidative mechanisms (15–17). From this evaluation, marker peptides for damage tracking were selected. The criteria utilized for the selection of markers were as follows:

- The peptide contained a photosensitive aromatic residue: phenylalanine, tyrosine, tryptophan, and/or histidine.
- The peptide was reproducibly observed in ESI-MS analysis of the unfractionated keratin tryptic digests with a high relative ion intensity.
- The peptide ion  $m/z$  and the  $m/z$  of corresponding major photoproduct ions were clear of interfering ions in the unfractionated analysis.

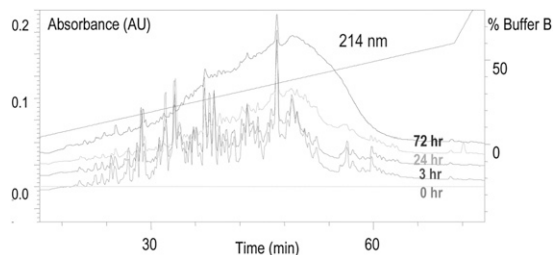


**Figure 1.** HPLC traces of keratin digest solutions corresponding to UVA irradiation times of 0, 3, 24, and 72 h (monitored at 214 nm).

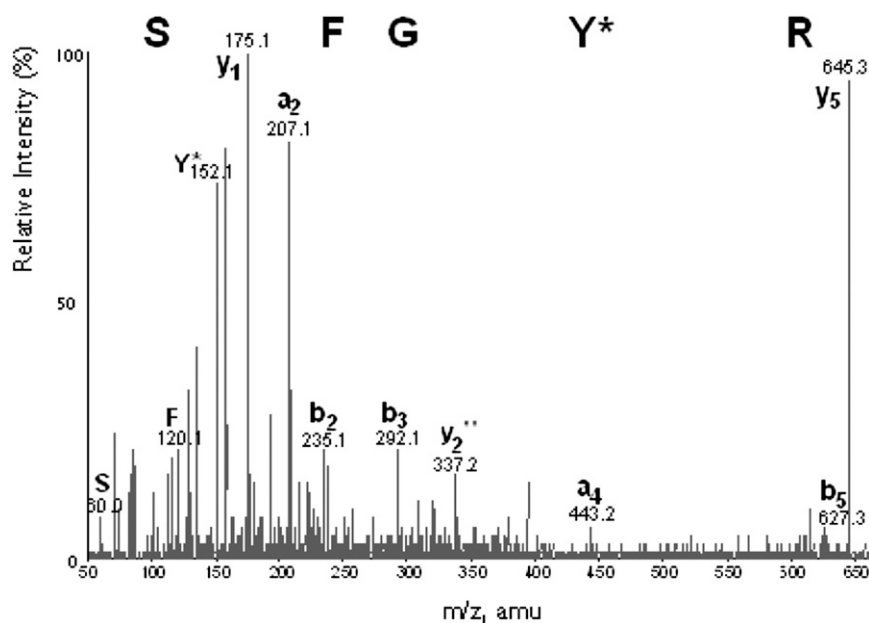


Figure 2. ESI-MS/MS spectrum of the keratin-derived peptide SFGY\*R ( $m/z$  645.3), where tyrosine (Y) has been photomodified by UVA exposure to dihydroxyphenylalanine (dopa) (Y\*), with selected fragment ions highlighted.

An ESI-MS/MS spectrum showing tyrosine photooxidation in the keratin-derived peptide with native sequence SFGYR is shown in Figure 2. This peptide met the criteria for use as a molecular marker of redox damage. Using MS/MS fragmentation data, a range of photo-induced redox modifications were thus characterized and located within wool keratins. Those peptides meeting the criteria for potential utilization as redox damage markers are listed in Table I, along with observed UVA-induced photomodifications.

#### DAMAGE TRACKING

To validate redox damage tracking for keratins, the relative abundance of selected oxidative modifications to keratin marker peptides was evaluated over differing irradiation protocols. Parallel quantitative evaluation of both the ion intensity and the ion peak area of each oxidative damage product was performed relative to the unmodified native peptide within each sample, with each sample analyzed in triplicate. The two differing quantitative methods were employed in parallel both for comparison purposes and to demonstrate the validity of the marker peptide approach for both methods. This is summarized for two peptides identified as good candidates for use as molecular redox damage markers in Tables II and III.

In the keratin marker peptide SFGYR, blue light produced an initial increase in the relative abundance of the tyrosine primary oxidation products, dopa, likely due to the UV component of the blue light utilized (11), but this was subsequently photo-bleached by further irradiation, consistent with the absorption of blue light (i.e.,

**Table I**  
Summary of Selected Keratin Damage Marker Peptides and Their Observed UVA-induced Photomodifications. Modified Residues Are Marked in Bold

	Photomodification	Photoproduct	Marker peptide
Phenylalanine	Hydroxylation [+O]	Tyrosine	LQFFQNR LASDDFR
	Dihydroxylation [+2O]	Dopa	LQFFQNR FAAFIDKEIR
Tyrosine	Hydroxylation [+O]	Dopa	LASYLEK SFGYR
	Dihydroxylation [+2O]	Topa	SFGYR
Tryptophan	Hydroxylation [+O]	Hydroxytryptophan	DVEEWYIR
	Oxidative ring opening [+2O]	N-Formylkynurenine	DVEEWYIR
	Oxidative ring opening [+2O], deformylation [-CO]	Kynurenine	DVEEWYIR

dopa acting as a yellow chromophore) leading to further modification. For UVA and UVB irradiation, the level of the oxidized marker peptide increased with irradiation time, with the native marker peptide being completely destroyed after 72 h of UVB irradiation. In the keratin marker peptide, LASDDFR, the damaged peptide in which the phenylalanine residue was oxidized to tyrosine was found to increase steadily both during UVA and UVB, and blue light irradiation, consistent with the initial photoproduct, tyrosine, absorbing only UV light, and therefore not photobleaching in blue light.

The photobleaching effect of blue light on protein-bound chromophores formed through UV exposure, of particular relevance to the indoor light stability of carpet

**Table II**

Dopa Formation From Tyrosine in the Keratin Wool Peptide, SFGYR (Unmodified Tyrosine  $m/z$  629.3, Modified Dopa  $m/z$  645.3) After Blue Light, UVA or UVB Irradiation, Expressed as the Abundance of the Modified Peptide Relative to the Unmodified Peptide, as Assessed Using Ion Peak Intensity or Peak Area

Treatment	Peak intensity			Peak area		
	$m/z$ 629.3	$m/z$ 645.3	Y*:Y	$m/z$ 629.3	$m/z$ 645.3	Y*:Y
<b>Blue Light</b>						
3 h	11,114	464	4.2	756.467	51.526	6.8
24 h	1,668	407	24.4	145.956	46.665	32.0
72 h	3,363	174	5.2	225.219	20.098	8.9
<b>UVA</b>						
3 h	9,685	1,168	12.1	755.166	150.045	19.8
24 h	11,256	2,537	22.5	1,000.694	330.6521	33.0
72 h	908	435	47.9	82.756	40.423	48.8
<b>UVB</b>						
3 h	1,659	273	16.5	144.962	25.876	17.9
24 h	434	551	127.0	55.983	63.704	113.3
72 h	N/A	N/A		N/A	N/A	

Sequence: SFGYR; Location: K2M2 res 62-661; Modification: Y→[Y+O]. Y\* is the modified residue.

Table III

Dopa Formation From Tyrosine in the Keratin Wool Peptide, LASDDFR (Unmodified Tyrosine  $m/z$  823.4, Modified Dopa  $m/z$  839.4) After Blue Light, UVA or UVB Irradiation, Expressed as the Abundance of the Modified Peptide Relative to the Unmodified Peptide, as Assessed Using Ion Peak Intensity or Peak Area

Treatment	Peak intensity			Peak area		
	$m/z$ 823.4	$m/z$ 839.4	F*:F	$m/z$ 823.4	$m/z$ 839.4	F*:F
<b>Blue light</b>						
3 h	226	152	67.3	26.2039	20.8936	79.7
24 h	64	59	92.2	8.3824	8.2307	98.2
72 h	97	125	128.9	10.9161	14.9627	137.1
<b>UVA</b>						
3 h	1332	1079	81.0	208.2376	173.0123	83.1
24 h	283	284	100.4	45.3400	46.4632	102.5
72 h	44	66	150.0	4.1464	5.7242	138.1
<b>UVB</b>						
3 h	103	47	45.6	11.3387	4.7810	42.2
24 h	104	111	106.7	12.6693	17.5339	138.4
72 h	94	156	166.0	9.1246	16.7719	183.8

Sequence: LASDDFR; Location: K1M2 res 135-141; Modification: F→Y. F\* is the modified residue.

wools, was further investigated at the molecular marker level through sequential irradiation first with UVA and then with blue light. The results for a keratin marker peptide containing tryptophan are shown in Table IV, showing an initial UV-induced increase in the relative abundance of the photoproduct, kynurenine, followed by a decrease in the relative abundance after blue light photobleaching. These results demonstrate the utility of marker peptides in proteomic characterization and tracking of redox damage in keratins.

Table IV

Kynurenine Formation from Tryptophan in the Keratin Wool Peptide, DVEEWYIR (Unmodified  $m/z$  1109.5, Modified  $m/z$  1113.5) After 24 h UVA Irradiation and Varying Periods of Blue Light Irradiation, Expressed as the Abundance of the Modified Peptide Relative to the Unmodified Peptide, as Assessed Using Ion Peak Intensity or Peak Area

Treatment	Peak intensity			Peak area		
	$m/z$ 1109.5	$m/z$ 1113.5	W*:W	$m/z$ 1109.5	$m/z$ 1113.5	W*:W
<b>UVA</b>						
24 h	166	63	38.0	28.5065	11.3454	39.8
<b>24 h UVA + blue light</b>						
24 h	43	40	93.0	2.1699	3.5685	164.5
48 h	2193	745	34.0	769.7623	328.7012	42.7
72 h	1670	537	32.2	286.9957	96.5852	33.7

Sequence: DVEEWYIR; Location: K1M1, K1M2 res 241-248; Modification: W→[W+2O-CO]. W\* is the modified residue.

**Table V**  
Change in Yellowness (Y-Z) in Wool Fabric Irradiated for 72 h with UVA, UVB, or Blue Light, with Statistical Error Presented as One Standard Deviation (SD)

Irradiation type	Y-Z score	SD
Control (unirradiated)	7.73	0.70
UVA	13.57	0.80
UVB	22.79	1.54
Blue	6.40	0.49

APPLICATION TO A COMPLEX PROTEIN SYSTEM: DAMAGE AND PROTECTION OF WHOLE WOOL

The next step was to apply and validate the tracking of redox modification in marker peptides to a complex proteinaceous system, in this case wool fabric. The dry weight of wool comprises approximately 98% proteins, with about 60% of the total weight being derived from keratins (18,19). The keratins are also the key structural proteins in skin,

**Table VI**  
Keratin Photomodifications Characterized in 72 h UVA Irradiated Whole Wool (Modified residues underlined)

Monoisotopic <i>m/z</i>	Charge	Sequence	Modification
<b>Tryptophan</b>			
854.34	1+	AEAEAW <u>Y</u>	Oxidation (W)
Protein ID		Type II K82	
855.33	1+	DVEEW <u>Y</u>	Oxidation (W)
Protein ID		Type I K31K33a, K33b, K34	
1200.53	2+	<u>W</u> QFYQNQR	Formylkynurenine (W)
Protein ID		Type II K85	
1867.68	3+	SCN <u>W</u> FC <del>E</del> GSFDGNEK	Formylkynurenine (W), Carbamidomethyl (C)
Protein ID		Type I K31, K33a, K33b, K34	
721.26	1+	AEAES <u>W</u>	Tryptophandione (W)
Protein ID		Type II K81, K83, K85, K86, K87	
747.28	1+	AEVES <u>W</u>	Bis-tryptophandione
Protein ID		Type II K85( <i>Bos taurus</i> )	
1220.62	2+	LLETK <u>W</u> QLY	Bis-tryptophandione
Protein ID		Type II K85, K87	
<b>Tyrosine</b>			
966.46	2+	<u>LY</u> EEEEIR	Hydroxylation (Y)
Protein ID		Type II K81, K86, K87	
982.45	2+	<u>LY</u> EEEEIR	Dihydroxylation (Y)
Protein ID		Type II K81, K86, K87	
1023.48	2+	<u>Y</u> EEEEVALR	Hydroxylation (Y)
Protein ID		Type II K81, K85, K86	
1053.47	2+	AQ <u>Y</u> DDIASR	Hydroxylation (Y)
Protein ID		Type II K81, K83K85	
1069.45	2+	AQ <u>Y</u> DDIASR	Dihydroxylation (Y)
Protein ID		Type II K81, K83, K85	
1151.58	2+	K <u>Y</u> EEEEVALR	Hydroxylation (Y)



Table VI  
Continued

Monoisotopic <i>m/z</i>	Charge	Sequence	Modification
Protein ID 1179.57	2+	Type II K85 K <u>Y</u> EQEVALR	Nitration (Y)
Protein ID 1179.58	2+	Type II K83 R <u>Y</u> EEEEVALR	Hydroxylation (Y)
Protein ID 1195.57	2+	Type II K81, K86 R <u>Y</u> EEEEVALR	Dihydroxylation (Y)
Protein ID 1240.62	2+	Type II K81, K86 TK <u>Y</u> ETEVSLR	Hydroxylation (Y)
Protein ID		Type I K33a	
Phenylalanine			
822.38	2+	LAADD <u>F</u> R	Hydroxylation (F)
Protein ID 838.37	2+	Type I K31, K32, K33b, K35, K38 LAADD <u>F</u> R	Dihydroxylation (F)
Protein ID 1037.50	2+	Type I K31, K32, K33b, K35, K38 AKLAADD <u>F</u> R	Dihydroxylation (F)
Protein ID		Type I K31, K33b, K35	
Others			
719.33	1+	<u>N</u> AQ <u>C</u> VK	Deamidation (N), carbamidomethyl (C)
Protein ID 972.49	2+	Type II K81, K83, K85, K86 LLEGQ <u>E</u> QR	Deamidation (Q)
Protein ID 974.49	2+	Type II K81 LTAEVEN <u>A</u> AK	Deamidation (N)
Protein ID 984.43	2+	Type II K81, K83, K86 EH <u>V</u> EADGGR	Oxidation (H)
Protein ID 999.56	1+	Type II K85 ( <i>Bos taurus</i> ) LVVQID <u>N</u> AK	Deamidation (N)
Protein ID 1031.51	2+	Type I K31, K33a, K33b, K35, Type I K33a QEEKEQ <u>I</u> K	Deamidation (Q)
Protein ID 1141.65	2+	Type II K81, K83, K86 LI <u>H</u> EINFLK	Oxidation (H)
Protein ID 1243.64	2+	Type II K82 ( <i>Bos taurus</i> ) QLVESD <u>I</u> NGLR	Deamidation (N)
Protein ID 1366.71	2+	Type I K31, K33b LASELN <u>H</u> VQEVL	Oxidation (H)
Protein ID 1399.74	2+	Type II K87 QLVESD <u>I</u> NGLRR	Deamidation (N)
Protein ID 1624.82	2+	Type I K31, K33b LNVEVDA <u>A</u> PPVDLNK	Hydroxylation (P)
Protein ID		Type I K36 ( <i>Bos taurus</i> )	
Backbone cleavage			
839.33	1+	DVEEWY	None
Protein ID 854.34	1+	Type I K31K33a, K33b, K34 AEAESWY	None
Protein ID		Type II K81, K83, K85, K86, K87	

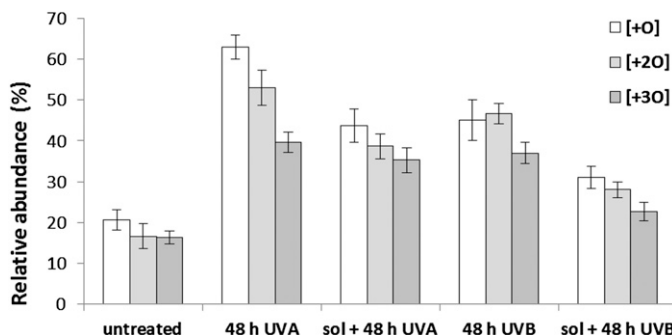


**Figure 3.** Comparative tracking of the levels of UVA- and UVB-induced modifications to tyrosine ( $Y \rightarrow [Y+O]$ ,  $[Y+2O]$ , and  $[Y+3O]$ ) in the marker peptide SFGYR ( $m/z$  629.3). The relative percentage indicates the peak area of SFG $[Y+O]$ R, SFG $[Y+2O]$ R, or SFG $[Y+3O]$ R relative to the SFGYR peak area in MS. Triplicate technical repeats were performed, with standard deviation indicated.

hair, and nails, and keratin marker peptides therefore represent an excellent target for proteomic evaluation of damage and protection at the molecular level. For comparison purposes, the yellowness of whole wool irradiated with our protocols was evaluated, and the Y-Z color scores are summarized in Table V.

Wool fabric was first irradiated with UVA for 72 h, and a complete redox proteomic profile compiled through LC-MS/MS analysis. In the case of wool irradiation, modifications associated with coloration changes are of particular interest, and so all oxidative modifications to the aromatic amino acid residues were identified. The full modification list is shown in Table VI. This proteomic profiling enabled full profiling of protein oxidative damage throughout the wool keratins, with characterization of specific higher abundance modifications for tracking.

An ESI-MS/MS-based proteomic evaluation was then performed with and without the application of a protective solgel surface treatment to the wool prior to 48 h UVA and UVB irradiation. Photomodifications corresponding to  $[+O]$ ,  $[+2O]$ , and  $[+3O]$  for tyrosine, and  $[+O]$  and  $[+2O]$  for tryptophan in keratin marker peptides were tracked proteomically. Figures 3 and 4 show the observed results for the two keratin marker peptides, SFGYR and DVEEWYIR.

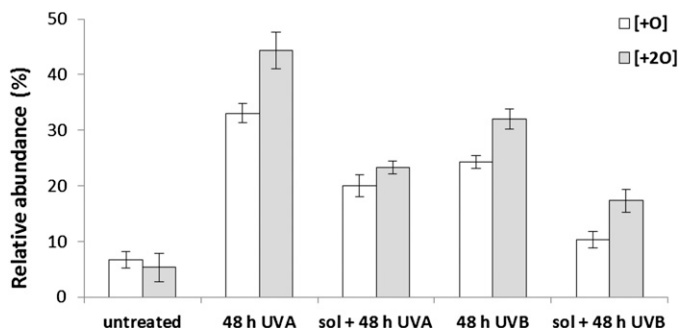


**Figure 4.** Comparative tracking of the levels of UVA- and UVB-induced modifications to tryptophan ( $W \rightarrow [W+O]$  and  $[W+2O]$ ) in the marker peptide DVEEWYIR ( $m/z$  1109.6). The relative percentage indicates the peak area of DVEEW $[W+O]$ YIR or DVEEW $[W+2O]$ YIR relative to DVEEWYIR peak area in MS. Triplicate technical repeats were performed, with standard deviation indicated.

Both wool damage marker peptides, SFGYR and DVEEWYIR, underwent significant photooxidative modification under UVA and UVB irradiation, evidenced by decreases in the abundance of MH<sup>+</sup> ions at *m/z* 629.3 and 1109.6, and corresponding increases in the relative abundance of their oxidized products. The relative increases of SFGY\*R Y+O, Y+2O, and Y+3O and of DVEEW\*IR W+O and W+2O provided an indication of the level of specific protection conferred by the treatment. Oxidation of the two native marker peptides was minimized in the samples with solgel surface treatment.

In addition to demonstrating the UV-protective effect of a silicon-based solgel matrix surface coating for wool at the molecular level, this evaluation validated the utility of marker peptides for characterizing and tracking redox damage and the effects of protective treatments on these factors, even within a complex proteinaceous system.

## CONCLUSIONS

This study has demonstrated and validated the utilization of marker peptides for profiling and tracking redox modification, as well as evaluating and validating protection or repair treatments. These are two valuable goals for hair and skin research and development.

Six marker peptides, five containing tyrosine and one containing tryptophan, were identified and validated through the evaluation of light-induced oxidative damage in an enriched keratin preparation. A full redox proteomic evaluation of UVA photomodification to aromatic residues in whole wool was successfully performed, with mapping of a wide range of modifications through the wool proteome. Subsequently, two selected keratin marker peptides, SFGYR and DVEEWYIR, were utilized both to track oxidative modification in whole wool through a range of UV irradiation protocols and to demonstrate the UV-protective effect of a prior solgel surface treatment of wool at the molecular level.

The utilization of such marker peptides has the potential for a range of cosmetic applications in hair, skin, and nails, in addition to applications tracking redox modification in protein foods and biomaterials. We anticipate that further development of this redox proteomic marker approach will allow more targeted design and evaluation of protection and repair treatments for protein systems, through mapping the type and location of damage at the molecular level.

## ACKNOWLEDGMENTS

We gratefully acknowledge support for this work from Wool Research Inc. (05WRCN03/08WRAG01) and the New Zealand Foundation for Research Science and Technology (C10X0710).

## REFERENCES

- (1) D. S. Fudge, T. Winegard, R. H. Ewoldt, D. Beriault, L. Szewciw, and G. H. McKinley, From ultra-soft slime to hard [alpha]-keratins: The many lives of intermediate filaments, *Integr. Comp. Biol.*, **49**, 32–39 (2009).
- (2) C. Popescu and H. Höcker, "Chapter 4: Cytomechanics of Hair: Basics of the Mechanical Stability," in *International Review of Cell and Molecular Biology*, W. J. Kwang. Ed. (Academic Press, London, 2009), pp. 137–156.

- (3) K. R. Millington and J. S. Church, The photodegradation of wool keratin II. Proposed mechanisms involving cystine, *J Photochem Photobiol B.*, **39**, 204–212 (1997).
- (4) R. H. Bradley, I. L. Clackson, and D. E. Sykes, UV ozone modification of wool fibre surfaces, *Appl Surf Sci.*, **72**, 143–147 (1993).
- (5) D. Yilmazer and M. Kanik, Bleaching of wool with sodium borohydride, *J Eng Fiber Fabr.*, **4**, 45–50 (2009).
- (6) J. M. Dyer, J. Plowman, G. Krsinic, S. Deb-Choudhury, H. Koehn, K. Millington, et al., Proteomic evaluation and location of UVB-induced photo-oxidation in wool, *J Photochem Photobiol B.*, **98**, 118–127 (2010).
- (7) J. M. Dyer, S. Bringans, and W. G. Bryson, Characterisation of photo-oxidation products within photoyellowed wool proteins: Tryptophan and tyrosine derived chromophores, *Photochem Photobiol Sci.*, **5**, 698–706 (2006).
- (8) B. Mahltig, F. Audenaert, and H. Bottcher, Hydrophobic silica sol coatings on textiles—The influence of solvent and sol concentration, *J Sol-Gel Sci Technol.*, **34**, 103–109 (2005).
- (9) Technical release: Luzchem exposure standard: LES-UVA-01 (2004) Available from: <http://www.luzchem.com/handbook/LESUVA011.pdf>.
- (10) Technical release: Luzchem exposure standard: LES-UVB-01 (2004) Available from: <http://www.luzchem.com/handbook/LESUVB011.pdf>.
- (11) Technical release: Luzchem exposure standard: LES-420-01 (2004) Available from: <http://www.luzchem.com/handbook/LES420011.pdf>.
- (12) H. Thomas, A. Conrads, K. H. Phan, M. van de Löcht, and H. Zahn, In vitro reconstitution of wool intermediate filaments, *Int J Biol Macromol.*, **8**, 258–264 (1986).
- (13) N. R. Parker, J. F. Jamie, M. J. Davies, and R. J. W. Truscott, Protein-bound kynurenine is a photosensitizer of oxidative damage, *Free Radic Biol Med.*, **37**, 1479–1489 (2004).
- (14) A. Pirie, Formation of N'-formylkynurenine in proteins from lens and other sources by exposure to sunlight, *Biochem J.*, **125**, 203–208 (1971).
- (15) T. Gensch, J. Hendriks, and K. J. Hellingwerf, Tryptophan fluorescence monitors structural changes accompanying signalling state formation in the photocycle of photoactive yellow protein, *Photochem Photobiol Sci.*, **3**, 531–536 (2004).
- (16) J. Lee, N. Koo, and D. B. Min, Reactive oxygen species, aging, and antioxidative nutraceuticals, *Compr Rev Food Sci Food Saf.*, **3**, 21–33 (2004).
- (17) C. Wei, B. Song, J. Yuan, Z. Feng, G. Jia, and C. Li, Luminescence and Raman spectroscopic studies on the damage of tryptophan, histidine and carnosine by singlet oxygen, *J Photochem Photobiol A Chem.*, **189**, 39–45 (2007).
- (18) J. A. Maclaren and B. Milligan, "The Structure and Composition of Wool," In *Wool Science—The Chemical Reactivity of the Wool Fibre* (Science Press, Marrickville, Australia, 1981), pp. 1–18.
- (19) R. C. Marshal, D. F. G. Orwin, and J. M. Gillespie, Structure and biochemistry of mammalian hard keratin, *Electron Microsc Rev.*, **4**, 47–83 (1991).